J. Fluid Mech. (1971) *vol.* 46, *part* 1, *pp.* 65–81
Printed in Great Britain

Convection in a rotating annulus uniformly heated from below

By ROBERT P. DAVIES-JONES
AND PETER A. GILMAN

Advanced Study Program,
National Center for Atmospheric Research
Boulder, Colorado

(Received 8 April 1970)

We present a linear stability analysis, to second order in initial amplitude, of Bénard convection of a Boussinesq fluid in a thin rotating annulus for modest Taylor numbers T ($\leqslant 10^4$). The work is motivated in part by the desire to study further a mechanism for maintaining, through horizontal Reynolds stresses induced in the convection, the sun's 'equatorial acceleration', which has been demonstrated for a rotating convecting spherical shell by Busse & Durney. The annulus is assumed to have stress free, perfectly conducting top and bottom (which allows separation of the equations) and non-conducting *non*-slip sides. A laboratory experiment which fulfills these conditions (except perhaps the free bottom) is being developed with H. Snyder.

We study primarily annuli with gap-width to depth ratios a of order unity. The close, non-slip side-walls produce a number of effects not present in the infinite plane case, including overstability at high Prandtl numbers P, and multiple minima in Rayleigh number R on the stability boundary. The latter may give rise to vacillation. The eigenfunctions for stationary convection for $a = 2$, $T \lesssim 2000$ clearly show momentum of the same sense as the rotation is transported from the inner to the outer half of the annulus, corresponding to transport toward equatorial latitudes on the sphere. The complete second-order solutions for the induced circulations indeed give faster rotation in the outer half, except for large P ($> 10^2$), in which case thermal stresses dominate. At all P, this differential rotation is qualitatively a thermal wind. Overstable convective cells, and stationary cells at higher T, induce more complicated differential rotations.

1. Introduction and summary

Convection in a rotating annulus driven by an imposed *horizontal* (radial) temperature gradient has received much attention from geophysical fluid dynamicists, owing largely to its dynamical similarities to planetary scale flow in the terrestrial atmosphere and atmospheres of other planets. In contrast, annulus convection driven by an imposed *vertical* temperature gradient has been studied very little. This problem is, we feel, of interest for studying a possible mechanism for producing and maintaining the differential rotation of the sun.

The mechanism is basically this: due to Coriolis forces, convective motions in a rotating fluid possess non-zero Reynolds stresses which can redistribute the angular momentum of solid rotation to give differential rotation. This effect has been studied for convection in a spherical shell by Busse (1970) using a perturbation expansion model, and by Durney (1970) with a limited harmonic non-linear model. The writers have demonstrated the effect in the annulus for the case of an ideal (viscosity, thermal diffusivity equal to zero) unstably stratified fluid (Davies-Jones & Gilman 1970). We propose here to demonstrate this effect in a viscous, thermally conducting fluid contained in an annulus. We do this by means of a normal mode stability analysis carried to second order in perturbation amplitudes.

The thin annulus problem, in addition to being simpler mathematically than the spherical shell, also lends itself to analysis by laboratory experiment, although an important difficulty will be the simulation of a free bottom boundary. (Simulation of a free bottom has been done for the non-rotating convection problem by Goldstein & Graham 1969). Such an experiment is currently being built with H. Snyder, and will be reported on later.

The annulus gap-width is assumed small enough compared to its mean radius so that local Cartesian co-ordinates may be employed. Rotation is assumed small enough that centrifugal effects may be ignored. (We discuss the criteria for this in more detail in § 2.) The top and bottom are for simplicity assumed to be stress free and perfectly conducting, while the sides are insulating and non-slip. The fluid is also treated as Boussinesq. With these assumptions, the vertical, longitudinal and time dependence of the perturbations separate out easily, leaving ordinary differential equations in the radial or lateral co-ordinate y. These are solved by applying full-no-slip boundary conditions at the sides. This problem has been solved in the non-rotating case by Davies-Jones (1970).

Our analysis concentrates on annuli with gap-width to height ratios of order unity. The closeness of the no-slip side-walls gives rise to some new and interesting effects, not seen in the infinite plane case. For example, overstability is shown to occur at high Prandtl numbers as well as at low ones. Also, overstability sets in at relatively small Taylor numbers. The side-walls can actually be destabilizing at some Taylor numbers, counteracting the stabilizing effect of rotation. In general, the stability boundary is rather complicated, with multiple minima in the Rayleigh number as a function of longitudinal wave-number. For some Taylor numbers, two distinctly different wave-numbers become unstable at about the same Rayleigh number, suggesting the possibility of vacillation in a non-linear model or laboratory experiment. As still another effect, in some regions of the parameter space, the first and second stationary unstable modes coalesce into a pair of overstable modes. It is shown that this must occur at all Prandtl numbers.

In the spherical problem, Busse & Durney find that with rotation at modest Taylor numbers the most unstable mode is non-axisymmetric and extends from pole to pole, being bounded by meridians.† The Coriolis forces acting on these

† For the sun, if we are talking about global scale cells extending through the convection zone, which are acted upon in an eddy diffusive way by the much smaller scale granules and supergranules, then the appropriate Taylor number is $\lesssim 10^4$.

banana shaped 'rolls' cause them to concentrate angular momentum in equatorial regions. In the thin annulus, the most unstable modes without rotation are somewhat analogous, being nearly transverse rolls (Davies-Jones 1970). These modes, so long as they remain stationary, are distorted by Coriolis forces for Taylor numbers above about unity depending on aspect ratio. At small and moderate Prandtl number ($< 10^2$), and not too large Taylor number, they concentrate angular momentum in the outer half of the annulus cross section,† corresponding to equatorial latitudes on the sphere. The overstable and high Taylor number stationary modes produce more complicated differential rotations.

At large Prandtl numbers ($\gtrsim 10^2$), the thermal forcing dominates in determining the differential rotation in which case the average rotation of the inner and outer halves of the annulus is the same. For all P, the forced meridional circulation is thermally direct (warm fluid rising, cold sinking at the same level) and the differential rotation can be interpreted qualitatively as a 'thermal wind'.

It should be emphasized that the analogy between the thin annulus and the spherical shell is not precise, for at least two reasons. First, the spherical problem without rotation is degenerate in that no longitudinal wave-number is selected; in the annulus the side-walls do select a particular non-axisymmetric mode. Secondly, the spherical shell modes propagate in longitude like Rossby waves; in the annulus, any propagation is from the usual kind of convective overstability characteristic of the infinite plane models.

2. Basic equations and perturbation expansion

Let us scale all lengths with respect to the depth d of the annulus, with z as the dimensionless vertical co-ordinate, y the inward radial or lateral co-ordinate, and x parallel to the annulus walls. We define the ratio of gap width to depth to be a, and place the annulus in the range

$$-\tfrac{1}{2}a \leqslant y \leqslant +\tfrac{1}{2}a, \quad 0 \leqslant z \leqslant 1.$$

Therefore, $y = -\frac{1}{2}a$ corresponds to the outer rim of the annulus. Then we take κ to be the thermal diffusivity, ν the kinematic viscosity, βd the basic temperature difference between the bottom and top (assumed negative), α the coefficient of volume expansion, g gravity, acting in the negative z direction, and Ω the rotation rate about the z direction. We denote the dimensionless velocities (scaled by κ/d) by u, v, w in the x, y, z directions respectively, the time (scaled by d^2/κ) as t, the temperature deviation from linear by θ (scaled by $-\beta d$), and let π (scaled by κ^2/d^2) be the deviation from hydrostatic pressure divided by the mean density. (π also includes the centrifugal potential that is coupled with the mean density.) Then, if we define three dimensionless parameters in addition to the aspect ratio a, namely, the Rayleigh number R, the Prandtl number P and the Taylor number T, as

$$R = -\frac{g\alpha\beta d^4}{\kappa\nu}, \quad P = \frac{\nu}{\kappa}, \quad T = \frac{4\Omega^2 d^4}{\nu^2},$$

† Inner and outer halves of the annulus cross-section are unequivocally defined in the Cartesian limit when rotation is present.

and define $\mathbf{V} = u\mathbf{x} + v\mathbf{y} + w\mathbf{z}$, where $\mathbf{x}$, $\mathbf{y}$, $\mathbf{z}$ are the co-ordinate unit vectors, then the non-linear Boussinesq equations of motion, thermodynamics and continuity in the rotating system may be written as

$$\left(\frac{\partial}{\partial t} + \mathbf{V}.\boldsymbol{\nabla} - P\nabla^2\right) u = -\frac{\partial \pi}{\partial x} + PT^{\frac{1}{2}}v, \tag{1}$$

$$\left(\frac{\partial}{\partial t} + \mathbf{V}.\boldsymbol{\nabla} - P\nabla^2\right) v = -\frac{\partial \pi}{\partial y} - PT^{\frac{1}{2}}u, \tag{2}$$

$$\left(\frac{\partial}{\partial t} + \mathbf{V}.\boldsymbol{\nabla} - P\nabla^2\right) w = -\frac{\partial \pi}{\partial z} + PR\theta, \tag{3}$$

$$\left(\frac{\partial}{\partial t} + \mathbf{V}.\boldsymbol{\nabla} - \nabla^2\right) \theta = w, \tag{4}$$

$$\frac{\partial u}{\partial x} + \frac{\partial v}{\partial y} + \frac{\partial w}{\partial z} = 0. \tag{5}$$

The boundary conditions are, at top and bottom,

$$\frac{\partial u}{\partial z}, \frac{\partial v}{\partial z}, w, \quad \theta = 0; \quad z = 0, 1, \tag{6}$$

and, at the sides,

$$u, v, w, \quad \frac{\partial \theta}{\partial y} = 0, \quad y = \pm \tfrac{1}{2}a. \tag{7}$$

Let us now write each dependent variable as the sum of an axisymmetric basic state, which we denote by an overbar, and a perturbation or deviation from that state, which we denote by a prime. (The perturbations may also be axisymmetric although we will not be concerned with them in the second-order calculations, since they are not the most unstable first-order perturbations in the Cartesian limit; see §3(ii).) Then we assume that we have initially a basic state of rest relative to the rotating system, with hydrostatic balance in the vertical and a linear vertical temperature gradient, so that $u = \overline{u} = 0$, $v = \overline{v} = 0$, $w = \overline{w} = 0$, $\theta = \overline{\theta} = 0$, $\pi = \overline{\pi} = 0$. The initial growth of perturbations about this state, to first order in perturbation amplitude, is given, from (1)–(5), by

$$\left(\frac{\partial}{\partial t} - P\nabla^2\right) u' = -\frac{\partial \pi'}{\partial x} + PT^{\frac{1}{2}}v', \tag{8}$$

$$\left(\frac{\partial}{\partial t} - P\nabla^2\right) v' = -\frac{\partial \pi'}{\partial y} - PT^{\frac{1}{2}}u', \tag{9}$$

$$\left(\frac{\partial}{\partial t} - P\nabla^2\right) w' = -\frac{\partial \pi'}{\partial z} + PR\theta', \tag{10}$$

$$\left(\frac{\partial}{\partial t} - \nabla^2\right) \theta' = w', \tag{11}$$

$$\frac{\partial u'}{\partial x} + \frac{\partial v'}{\partial y} + \frac{\partial w'}{\partial z} = 0, \tag{12}$$

with the boundary conditions given by (6) and (7) with primes added.

Now, if these perturbations grow, i.e. if convection sets in, their Reynolds and thermal stresses will soon force, by non-linear interactions, changes in the basic state variables $\overline{u}, \overline{v}, \overline{w}, \overline{\theta}, \overline{\pi}$. By retaining products of perturbations in the expansion of (1)–(5), averaging these equations in x around the annulus, and dropping products of basic state variables, which are initially of fourth order, we can obtain equations for the *initial* forms of these forced changes, which are given by

$$\left(\frac{\partial}{\partial t} - P\overline{\nabla}^2\right)\overline{u} - PT^{\frac{1}{2}}\overline{v} = G_u, \tag{13}$$

$$\left(\frac{\partial}{\partial t} - P\overline{\nabla}^2\right)\overline{v} + \frac{\partial \overline{\pi}}{\partial y} + PT^{\frac{1}{2}}\overline{u} = G_v, \tag{14}$$

$$\left(\frac{\partial}{\partial t} - P\overline{\nabla}^2\right)\overline{w} + \frac{\partial \overline{\pi}}{\partial z} - PR\overline{\theta} = G_w, \tag{15}$$

$$\left(\frac{\partial}{\partial t} - \overline{\nabla}^2\right)\overline{\theta} - \overline{w} = G_\theta, \tag{16}$$

$$\frac{\partial \overline{v}}{\partial y} + \frac{\partial \overline{w}}{\partial z} = 0. \tag{17}$$

In the above, $\overline{\nabla}^2 = \partial^2/\partial y^2 + \partial^2/\partial z^2$, and the forcing functions G obtained from the stresses are defined as follows:

$$G_u = -\frac{\partial}{\partial y}\overline{u'v'} - \frac{\partial}{\partial z}\overline{u'w'}, \tag{18}$$

$$G_v = -\frac{\partial}{\partial y}\overline{v'^2} - \frac{\partial}{\partial z}\overline{v'w'}, \tag{19}$$

$$G_w = -\frac{\partial}{\partial z}\overline{w'^2} - \frac{\partial}{\partial y}\overline{v'w'}, \tag{20}$$

$$G_\theta = -\frac{\partial}{\partial y}\overline{v'\theta'} - \frac{\partial}{\partial z}\overline{w'\theta'}, \tag{21}$$

The boundary equations are again given by (6) and (7), this time with overbars applied.

We can see that, in general, the induced axisymmetric changes in the basic state are second order in perturbation amplitudes.

We still have to justify our neglect of centrifugal effects. For the basic state about which we perturb, we accept essentially the argument given by Greenspan (1968, pp. 12–14). That is, we assume gravity is very large compared to the centrifugal force, which, in a thin annulus of mean radius b, requires $Fa \ll 1$, where $F \equiv \Omega^2 b/g$ is a rotational Froude number. Then temperature and density in the basic state are essentially functions of height only, and the centrifugally induced circulation is very small. This assumption has been made in almost all preceding studies of convection in rotating fluids.

On the other hand, the centrifugal term may be neglected in the *perturbation* equations, if it is small compared to the Coriolis force in (9). This will be so if $T^{\frac{1}{2}} \gg FR_t$ provided that $|u'|/|\theta'| \gtrsim 1$ (we actually find in our solutions that $|u'|$

is always several times larger than $|\theta'|$). Thus, it is possible for centrifugal effects to be important in the perturbation equations, even though $Fa \ll 1$. Our calculations are for $T \leqslant 10^4$, $R \leqslant 5 \times 10^3$ with $10^3 \geqslant P \geqslant 10^{-3}$. With these limits, all centrifugal effects can be ignored for typical experimental fluids, such as water, air and mercury in an annulus of mean radius 16 cm, with aspect ratios of order unity.

3. First-order linear solutions

(i) *Solution procedure*

Separable solutions of the form

$$\left.\begin{matrix} u', v', \pi' \\ w', \theta' \end{matrix}\right\} = \left\{\begin{matrix} \hat{u}(y),\ \hat{v}(y),\ \hat{\pi}(y)\cos mz \\ \hat{w}(y), \hat{\theta}(y)\sin mz \end{matrix}\right\} \exp[\sigma t + ikx], \tag{22}$$

satisfy the boundary conditions at top and bottom. Substitution of (22) into (8)–(12), and elimination of variables, yields a single eighth-order equation in y for, say, the temperature, which if we assume

$$\hat{\theta} = \sum_{n=1}^{8} K_n e^{r_n y}, \tag{23}$$

reduces to a biquartic equation with roots r_n:

$$\sum_{q=0}^{4} X_{2q} r^{2q} = 0, \tag{24}$$

in which

$$\left.\begin{aligned} X_0 &= D^2 l^2 E + m^2 P^2 T E - PRDk^2, \\ X_2 &= PR(Pk^2 + D) - 2DPl^2 E - (E + l^2) D^2 - m^2 P^2 T, \\ X_4 &= l^2 E P^2 + D^2 + 2DP(E + l^2) - P^2 R, \\ X_6 &= -[2DP + P^2(E + l^2)], \\ X_8 &= P^2, \end{aligned}\right\} \tag{25}$$

and $$l^2 = k^2 + m^2, \quad D = \sigma + Pl^2, \quad E = \sigma + l^2.$$

Now, the boundary conditions at the sides can only be reduced to two variables, say $\hat{\theta}$ and $\hat{v}$:

$$\frac{\partial \hat{\theta}}{\partial y}, \quad \left(E - \frac{\partial^2}{\partial y^2}\right)\theta, \hat{v}, \quad \frac{\partial \hat{v}}{\partial y} = 0. \tag{26}$$

Therefore, we need an additional relation between $\hat{v}$ and $\hat{\theta}$. We choose

$$\begin{aligned} m\left[ik\left(D - P\frac{\partial^2}{\partial y^2}\right) - PT^{\frac{1}{2}}\frac{\partial}{\partial y}\right]\hat{v} \\ = \left[mPT^{\frac{1}{2}}\left(E - \frac{\partial^2}{\partial y^2}\right) - ik\left\{\left(D - P\frac{\partial^2}{\partial y^2}\right)\left(E - \frac{\partial^2}{\partial y^2}\right) - PR\right\}\frac{\partial}{\partial y}\right]\hat{\theta}, \end{aligned} \tag{27}$$

Since the perturbation equations (8)–(12) are linear and all operators commute, $\hat{v}$ must be of the same form as $\hat{\theta}$, i.e.

$$\hat{v} = \sum_{n=1}^{8} \alpha_n K_n e^{r_n y}, \tag{28}$$

where the α_n are determined by direct substitution of (23) and (28) into (27). Satisfaction of the boundary conditions (26) at the sides is ensured by the vanishing of the characteristic determinant of the eight equations for K_n:

$$\left.\begin{aligned} \sum_{n=1}^{8} r_n e^{\pm r_n \frac{1}{2}a} K_n = 0, \quad \sum_{n=1}^{8} (E - r_n^2) e^{\pm r_n \frac{1}{2}a} K_n = 0, \\ \sum_{n=1}^{8} \alpha_n e^{\pm r_n \frac{1}{2}a} K_n = 0, \quad \sum_{n=1}^{8} \alpha_n r_n e^{\pm r_n \frac{1}{2}a} K_n = 0. \end{aligned}\right\} \tag{29}$$

We consider only the lowest mode in the vertical, i.e. we set $m = \pi$ (this mode is by far the most unstable). We scan (judiciously) through a, R, P, T, k, σ space for the zeros of the determinant. We then find the constants K_n by Gaussian elimination. This gives us $\hat{\theta}$ and $\hat{v}$ from (23) and (28), and the other dependent variables can be obtained from (8) to (12).

(ii) *Stationary convection*

We limit our study to $T \leqslant 10^4$. Figure 1 gives the critical Rayleigh number as a function of Taylor number for different aspect ratios a. For a given a, R_c increases with T as in the infinite plane case. For walls closer together, one must

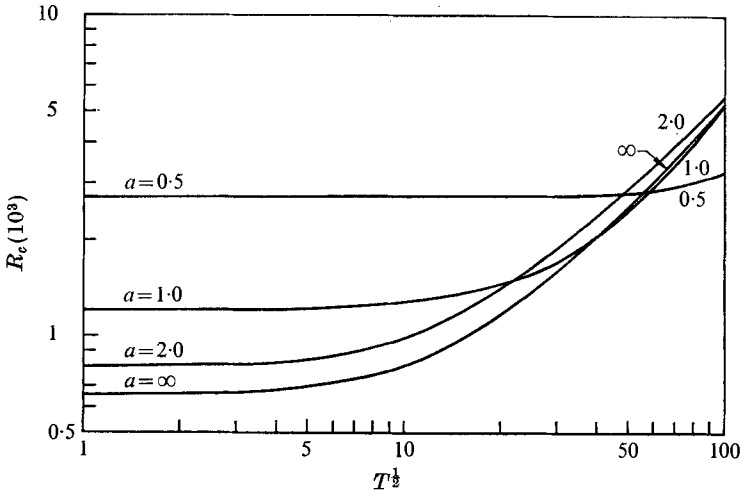

FIGURE 1. Critical Rayleigh number R_c *vs.* Taylor number T for various gap-width to depth ratios a.

go to higher Taylor numbers before rotation has an influence. This is clearly because, at low T, lateral diffusion of momentum to the side-walls dominates the Coriolis forces. As a consequence, bringing the walls closer together at some Taylor numbers is actually destabilizing as a result of the viscous forces releasing energy by inducing additional flow across the isobars. For example, for $T > 2500$ out to at least 10^4, we find R_c is less for $a = 0{\cdot}5$ than for $a = \infty$. Similarly, R_c is less for $a = 1$ than $a = 2$ above $T \approx 500$.

As in the non-rotating case (Davies-Jones 1970), the preferred mode at the onset of convection is non-axisymmetric in the Cartesian limit. This is in contrast

to the results of Koschmieder (1966) and Rossby (1969) for convection in a thin layer bounded laterally on the outside by a cylindrical wall. Presumably, in thicker annuli in which curvature is important, there is a transition to axisymmetric rolls.

In figure 2, we see that the critical wave-number k_c *generally* increases with T as in the $a = \infty$ case, but a sudden jump to lower k occurs for $a = 2{\cdot}0$ in the neighbourhood of $T = 2000$. This happens when a different local minimum of R

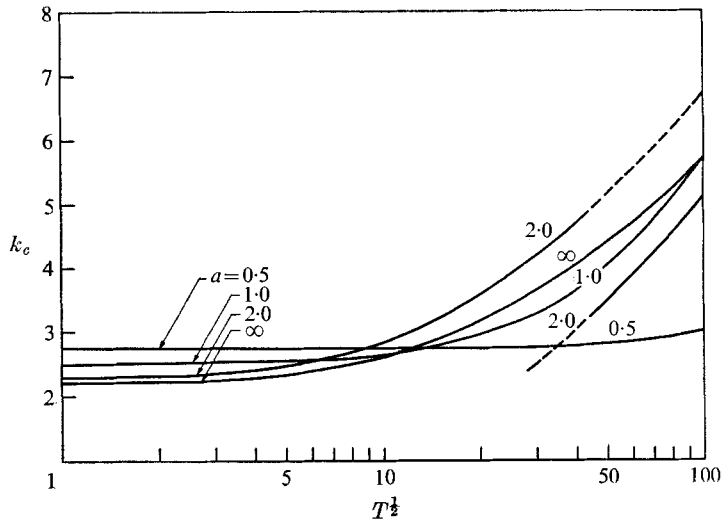

FIGURE 2. Critical azimuthal wave-number k_c *vs.* Taylor number T for various aspect ratios. Dashed extensions indicate k for local minimum in Rayleigh number R that is not the absolute minimum.

in the stationary stability boundary becomes the absolute minimum. (The stability boundary structure is discussed further below.) Which of the two distinctly different modes actually occurs in a non-linear model or experiment may be sensitive to initial conditions or previous history of the flow (or to temperature dependence of the diffusivities) and there may be vacillation between the two modes.

(iii) *Overstability*

The onset of overstability is demonstrated in figure 3, for $a = 2{\cdot}0$ and three Prandtl numbers $P = 7{\cdot}0$, $0{\cdot}7$, $0{\cdot}025$, corresponding approximately to water, air, and mercury. We note that overstability is predicted in both air and water, contrary to the infinite plane case. It sets in before stationary convection at $T \gtrsim 120$ for air, and $T \gtrsim 200$ for water. Also, mercury becomes overstable at a considerably lower Taylor number (≈ 100) than it does without side-walls (≈ 600).

The critical wave-number for overstability for the three Prandtl numbers, in general, increases less rapidly with T than for stationary convection, as without side-walls. On the other hand, k_c actually decreases with T for mercury.

Clearly, overstability will be pushed to higher Rayleigh numbers for small a due to the viscous side-walls overpowering the Coriolis forces, and we know it does not occur first at any R with $P > 0{\cdot}677$ for very large a (Chandrasekhar 1961). Thus there should be, for each P, an optimum aspect ratio for the occurrence of overstability.

As interpreted by Veronis (1966), overstability arises first above a certain Taylor number in low Prandtl number fluids so that the Coriolis forces can be balanced largely by local accelerations, allowing the pressure forces, which in steady convection would partially balance the Coriolis forces, to do more work

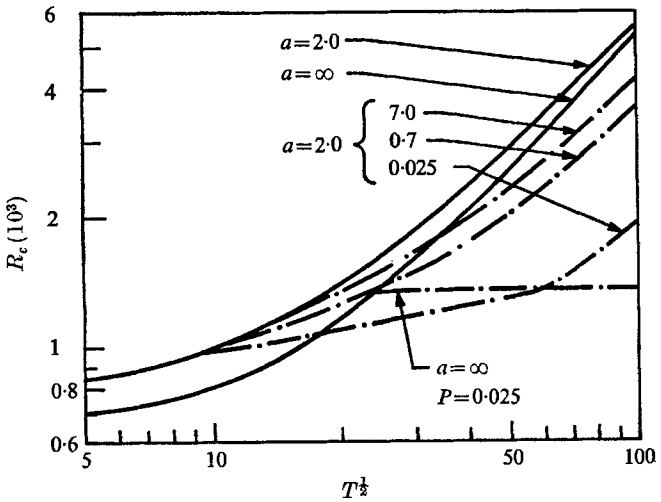

FIGURE 3. R_c for stationary convection (——) and overstable convection (—·—) for an aspect ratio $a = 2{\cdot}0$, ∞ and Prandtl numbers $P = 7{\cdot}0, 0{\cdot}7, 0{\cdot}025$.

against frictional dissipation. Since there is more dissipation with side-walls than without, overstability should cut in at a lower Taylor number, so long as Coriolis forces are not overpowered everywhere by the viscous sides. Veronis argues that overstability is prevented for high P because with relatively small thermal diffusion w and θ would get out of phase, reducing potential energy release. Evidently, the side-walls constrain such phase shifts in the y direction enough that overstability can occur, but it still requires a higher T.

(iv) *Structure of the stability boundary*

In order to show more clearly how the local minima in Rayleigh numbers evolve, and how overstability sets in, it is necessary to examine the neighbourhood of the stability boundary $R(k)$ in some detail. Figures 4(*a*)–(*c*) give its structure for $a = 2{\cdot}0$ and $T = 1, 10, 100$, respectively.

At $T = 1$, the rotation has virtually no influence, and the boundaries for stationary convection ($\sigma = 0$, solid lines) are the same as those found by Davies-Jones (1970). In the regions I, only the lowest mode in y is unstable, while, in region II, there are two stationary unstable modes. Between $T = 1$ and 10, the two $\sigma = 0$ curves break at the cross-over point and reconnect in pairs

giving distinctly separate regions I (see figure 4(*b*)). These new boundaries are connected at their vertical points by a line on which, except at the ends, σ is non-zero but imaginary, i.e. a boundary for overstability (dot-dashed curve). For this

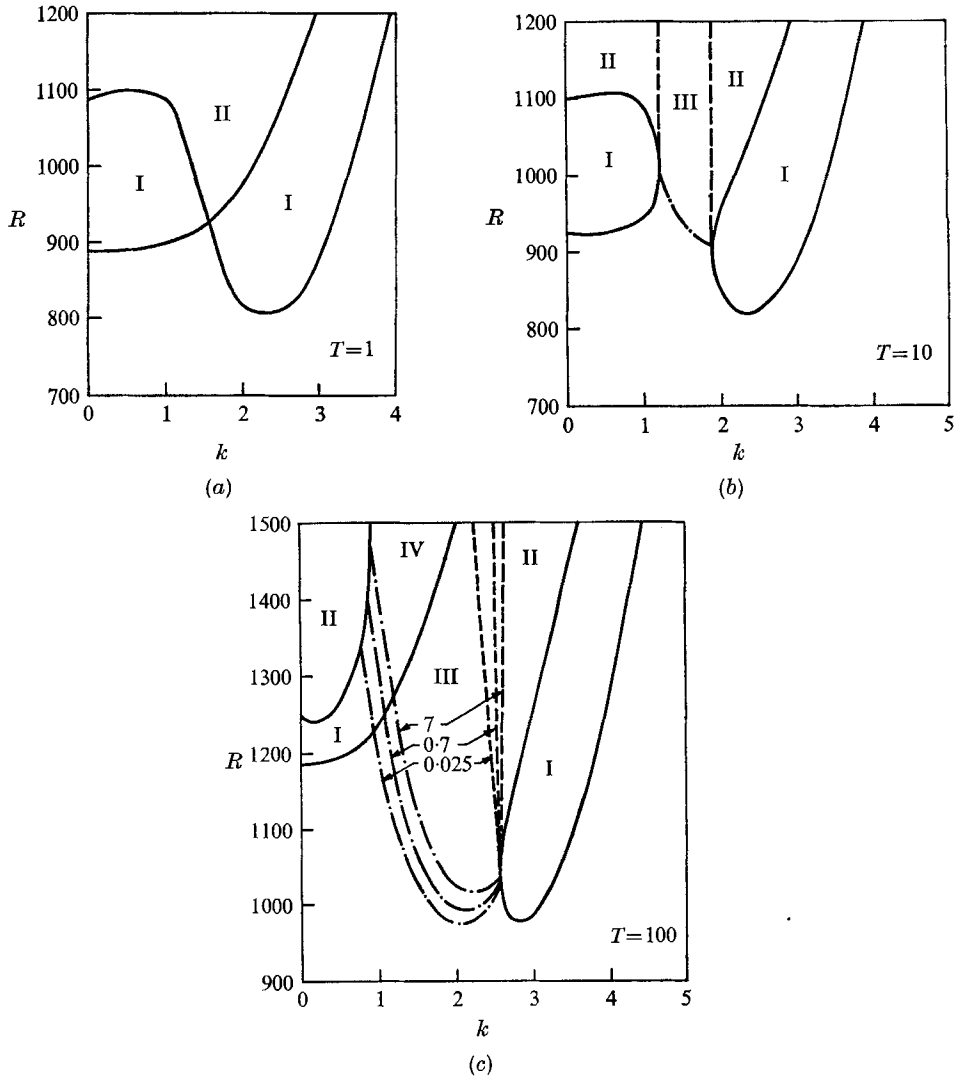

FIGURE 4. Structure of stability boundary for (*a*) $T = 1$, (*b*) $T = 10$, (*c*) $T = 100$. ——, boundaries for stationary convection; – – –, separation of two stationary unstable modes from two overstable modes; —·—, overstable convection boundaries. Regions I, lowest stationary unstable mode; II, two stationary unstable modes; III, two overstable modes; IV, two overstable and one stationary unstable mode.

small a Taylor number, the curves for $P = 0{\cdot}025$, $0{\cdot}7$, and 7 virtually coincide. Above this boundary, as one approaches either dashed line from regions II, the two stationary modes coalesce, reaching identical *non-zero* growth rate σ_r and structure on the dashed line. Crossing into region III, they acquire equal and opposite σ_i, but retain a common σ_r, corresponding to a pair of overstable modes.

Since the position of the stationary convection boundaries is independent of Prandtl number, it is clear from topological considerations that the overstable region III must exist in some form at all Prandtl numbers. This is quite different from the infinite plane case, for which no overstable modes exist at any R, T for $P > 1$ (Chandrasekhar 1961).

For still larger T, in particular $T = 100$ (figure 4(*c*)), the left-hand region I opens upward, and the overstable boundaries show significant Prandtl number dependence. Here, for mercury, overstable and stationary convection set in at virtually the same R, but distinctly different k. Therefore here, too, we have the possibility of vacillation, this time between a stationary and an overstable mode.

If we increase T still further, the two left-hand $\sigma = 0$ curves coalesce at one point, and then break as in figure 4(*b*) thereby forming a second 'finger shaped' region I with its own local minimum R and a new region of overstability. The right-hand finger moves to higher k, and the first overstability, remaining attached to the outermost finger drops down further relative to it, so that, as shown in figure 3, overstability sets in first.

As T is increased further yet, more and more new fingers are formed and migrate to higher k, etc. Although we have not carried the calculations this far, presumably the envelope of local minima approaches the stationary stability boundary for no side-walls at high T. The lower a is, the higher T at which the asymptotic form is effectively reached. At discrete points during this process, the critical Rayleigh number for stationary convection shifts to a new finger, giving rise to a sudden drop in k_c as seen in figure 2. In general, the further left a finger is, the more nodes the eigenfunctions have across the annulus.

We interpret this behaviour as follows: As T increases, it is harder to retain nearly transverse rolls, because Coriolis forces are producing cross annulus flow, first tilting the rolls and then deforming them into cells. The inhibiting effects of Coriolis forces should be minimized in cells whose x and y dimensions are comparable. Thus, as k_c increases with T, more nodes should appear across the annulus in the most unstable modes. Because of the side-walls, this adjustment can take place only in discrete jumps.

(v) *Structure of unstable modes*

A typical stationary convection cell structure in the rotating annulus is shown in figure 5 (horizontal section in the upper half) for the case $R = 1100$, $T = 100$, $k = 2{\cdot}8$, ($\sigma = 2{\cdot}0944$ for $P = 7{\cdot}0$), which is approximately the most unstable mode at about 10 % supercritical R. This close to R_c, the pattern is virtually independent of Prandtl number.

Without rotation, the cells are nearly transverse rolls (Davies-Jones 1970) at the onset of convection. Positive rotation, then, rotates the velocities and contours to the right, as we would expect. Looking at figure 5(*a*), it is immmediately evident from the tilt of the velocity vectors that the horizontal Reynolds stresses associated with the cells will transport momentum towards the outer rim of the annulus (corresponding to equatorward transport on the sphere); this is true at all levels except $z = \frac{1}{2}$, where the transport vanishes. Consequently, the outer half

of the fluid rotates faster, at the expense of the inner half. There will also, of course, be vertical structure in the induced differential rotation.

As the rotation is increased further, the stationary convection pattern breaks up into more and more cells between the annulus walls, as the absolute minimum R shifts from finger to finger.

The tilt of the cells at moderate T can be interpreted in terms of vorticity. Without rotation, the nearly transverse rolls have a large component of vorticity

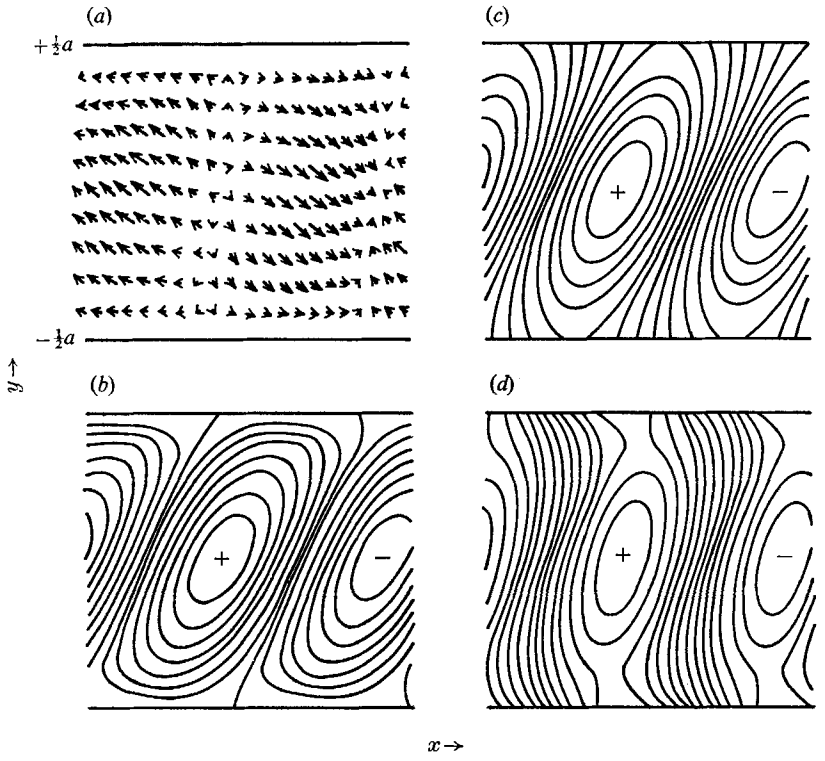

FIGURE 5. Structure of stationary convection cell looking down at upper half of annulus, for the case $T = 100, R = 1100, k = 2{\cdot}8, a = 2{\cdot}0$: (*a*) horizontal velocity vectors, (*b*) vertical motion, (*c*) temperature, (*d*) pressure contours. Patterns are virtually the same for all P in range $10^{-3} \leqslant P \leqslant 10^{+3}$ at least.

in the y direction. The x component of the vorticity equation predicts that through the term $+PT^{\frac{1}{2}}\,\partial u'/\partial z$, the y vorticity associated with $\partial u'/\partial z$ will be turned into the x direction by the Coriolis force so that, for $\partial u'/\partial z$ positive, the x vorticity induced is also positive. Thus the horizontal vorticity vector and consequently the convective roll are rotated or 'tilted' to the right. When the tilt gets sufficiently large, the roll is a less efficient converter of energy and so sets in at a higher Rayleigh number than a mode with less tilt but more nodes across the annulus.

For a given R, k, T, the two overstable cells, which propagate with equal speeds

in opposite directions along the annulus, have horizontal cell structures that are identical when one is rotated by 180° about the z direction. In the range

$$10^2 \leqslant T \leqslant 10^4,$$

these cells are highly asymmetric about $y = 0$, being concentrated near either the inner or the outer rim. The mode near the outer (inner) rim propagates in the negative (positive) x direction opposite to (in the same sense as) the basic rotation.

It is probable that effects not included in the linear stability theory will act to select the relative amplitudes of the two overstable modes. Thus, it is difficult to predict what the resulting observed circulation would look like.

4. Second-order solutions

(i) *Method of solution*

It is simplest to solve first for the forced mean meridional circulation $\bar{v}$, $\bar{w}$. If we define a stream function ψ such that $\bar{v} = \partial\psi/\partial z$, $\bar{w} = -\partial\psi/\partial y$, and let

$$\mathscr{L}_1 = \partial/\partial t - P\bar{\nabla}^2, \quad \mathscr{L}_2 = \partial/\partial t - \bar{\nabla}^2,$$

we may derive a single equation for ψ from (13) to (17), namely

$$\left(\mathscr{L}_1^2\mathscr{L}_2\bar{\nabla}^2 - PR\mathscr{L}_1\frac{\partial^2}{\partial y^2} + P^2T\mathscr{L}_2\frac{\partial^2}{\partial z^2}\right)\psi = F(y,z), \tag{30}$$

in which

$$F \equiv \mathscr{L}_1\mathscr{L}_2\left(\frac{\partial G_v}{\partial z} - \frac{\partial G_w}{\partial y}\right) - PR\mathscr{L}_1\frac{\partial G_\theta}{\partial y} - PT^{\frac{1}{2}}\mathscr{L}_2\frac{\partial G_u}{\partial z}. \tag{31}$$

If we use the boundary conditions on the perturbations to evaluate the forcing functions G at the boundaries, the boundary conditions on the second-order variables become

$$\frac{\partial\psi}{\partial y}, \quad \frac{\partial^2\psi}{\partial z^2}, \quad \mathscr{L}_1\bar{\nabla}^2\psi, \quad \mathscr{L}_1\bar{\nabla}^2\frac{\partial^2\psi}{\partial z^2} = 0 \quad (z = 0, 1), \tag{32}$$

$$\frac{\partial\psi}{\partial y}, \quad \frac{\partial\psi}{\partial z}, \quad \mathscr{L}_1\bar{\nabla}^2\psi, \quad \frac{\partial\bar{\theta}}{\partial y} = 0 \quad (y = \pm\tfrac{1}{2}a). \tag{33}$$

We should note here that the latter conditions require that $\partial\bar{u}/\partial z = 0$ at the sides but do not ensure that $\bar{u}$ itself vanishes. We return to this point later. As in the first-order problem, since not all the boundary conditions can be written in terms of ψ, we must solve (30) in conjunction with another equation relating ψ and $\bar{\theta}$. We take

$$\mathscr{L}_2\bar{\theta} + \frac{\partial\psi}{\partial y} = G_\theta \tag{34}$$

from (16).

Now, the second-order solutions are likely to resemble the full non-linear solutions only if we are close to the critical Rayleigh number (say, not more than 10 % above critical). We suppose, then, that near R_c it is the most unstable mode which eventually dominates. Therefore, we calculate the circulation forced by this mode. The solutions we find would apply if it is a stationary mode, or a single overstable

mode. We exclude from consideration the case of both overstable modes present at once.

For the above conditions, the convective cell doing the forcing is characterized by a single k, σ_r at a particular a, R, P, T. In that case, the forcing function F is of the form,

$$F = \sin 2mz\, e^{2\sigma_r t} \sum_{n,j=1}^{8} [F_{nj} \exp[(r_n + r_j^*)\, y] + F_{nj}^* \exp[(r_n^* + r_j)\, y]], \tag{35}$$

in which σ_r is the growth rate of the forcing cell, and r_n, r_j are the corresponding roots of (24). The asterisk denotes a complex conjugate. The forcing function,

$$\begin{aligned} F_{nj} = {} & [P(r_n + r_j^*)^4 - (2\sigma_r(1+P) + 8m^2P)\,(r_n + r_j^*)^2 + 4(\sigma_r^2 + 2m^2\sigma_r(1+P) + 4Pm^4)] \\ & \times [-2mV_{nj} - (r_n + r_j^*)\, W_{nj}] + PR[P(r_n + r_j^*)^2 - 2(\sigma_r + 2Pm^2)]\,(r_n + r_j^*)\,\theta_{nj} \\ & - 2mPT^{\frac{1}{2}}[(r_n + r_j^*) - 2(\sigma_r + 2m^2)]\, U_{nj}, \end{aligned}$$

in which

$$\begin{aligned} U_{nj} &= -\tfrac{1}{8}[(r_n + r_j^*)\, u_n v_j^* + 2mu_n w_j^*], \\ V_{nj} &= -\tfrac{1}{8}[(r_n + r_j^*)\, v_n v_j^* + 2mv_n w_j^*], \\ W_{nj} &= -\tfrac{1}{8}[(r_n + r_j^*)\, v_n w_j^* + 2mw_n w_j^*], \\ \theta_{nj} &= -\tfrac{1}{8}[(r_n + r_j^*)\, v_n \theta_j^* + 2mw_n \theta_j^*], \end{aligned}$$

where the first-order solutions are written in the form,

$$\hat{u}, \hat{v}, \hat{w}, \hat{\theta}(y) = \sum_{n=1}^{8} (u_n, v_n, w_n, \theta_n)\, e^{r_n y}.$$

The general solutions of (30) and (34) are given by $\psi = \psi_H + \psi_I$ and $\bar{\theta} = \bar{\theta}_H + \bar{\theta}_I$, where ψ_I and $\bar{\theta}_I$ are particular solutions to (30) and (34), ψ_H is the general solution of (30) with the right-hand side put equal to zero and $\bar{\theta}_H$ is the general solution of (34) with ψ replaced by ψ_H and G_θ by 0. From (30)

$$\psi_H = \sum_{j=1}^{8} C_j e^{s_j y} \sin 2mz\, e^{2\sigma_r t}, \tag{36}$$

where the s_j are the roots of $\sum_{q=0}^{4} X'_{2q} s^{2q} = 0$, the X'_{2q} being defined by (25) with $k = 0$, σ replaced by $2\sigma_r$ and m replaced by $2m$. A particular integral of (30) is

$$\psi_I = \sin 2mz\, e^{2\sigma_r t} \sum_{n,j=1}^{8} (\psi_{nj} \exp[(r_n + r_j^*)\, y] + \psi_{nj}^* \exp[(r_n^* + r_j)\, y]), \tag{37}$$

where $\psi_{nj} = F_{nj}/\Gamma_{rj}$, $\Gamma_{nj} = \sum_{q=0}^{4} X'_{2q}(r_n + r_j^*)^{2q}$. Similarly, from (34),

$$\bar{\theta}_H = \sum_{j=1}^{8} C_j \beta_j e^{s_j y} \sin 2mz\, e^{2\sigma_r t}, \tag{38}$$

where $\beta_j = -s_j/(2\sigma_r - s_j^2 + 4n^2)$ and

$$\bar{\theta}_I = \sin 2mz\, e^{2\sigma_r t} \sum_{n,j=1}^{8} [\bar{\theta}_{nj} \exp[(r_n + r_j^*)\, y] + \bar{\theta}_{nj}^* \exp[(r_n^* + r_j)\, y]], \tag{39}$$

where

$$\bar{\theta}_{nj} = [\theta_{nj} - \psi_{nj}(r_n + r_j^*)]/[2\sigma_r - (r_n + r_j^*)^2 + 4m^2].$$

The above solutions satisfy the boundary conditions (32) at top and bottom for all C_j. The C_j's are then determined by substitution of (36)–(39) into the side conditions (33) and solving by Cramer's rule.

Given that we know ψ and $\bar{\theta}$, we may find the induced differential rotation $\bar{u}$ from (13), if we require that $\bar{u} = 0$ at the sides (remember that the conditions (33) only required $\partial\bar{u}/\partial z = 0$ at the sides). A particular integral of (13) is

$$\bar{u}_I = \Big\{\cos 2mz \sum_{n,j=1}^{8} (\bar{u}_{nj}^{(1)} \exp[(r_n + r_j^*)\, y] + \bar{u}_{nj}^{(1)*} \exp[(r_n^* + r_j)\, y]) + \sum_{n,j=1}^{8} (\bar{u}_{nj}^{(2)} [\exp(r_n + r_j^*)\, y] + \bar{u}_{nj}^{(2)*} \exp[(r_n^* + r_j)\, y])\Big\} e^{2\sigma_r t}, \tag{40}$$

in which $$\bar{u}_{nj}^{(1)} = (U_{nj} + 2mPT\psi_{nj})/(2\sigma_r - P(r_n + r_j^*)^2 + 4m^2 P),$$

and $$\bar{u}_{nj}^{(2)} = -\tfrac{1}{8}(r_n + r_j^*)\, u_n v_j^*/(2\sigma - P(r_n + r_j^*)^2).$$

Now $\bar{u} = \bar{u}_H + \bar{u}_I$, where $\bar{u}_H$, the general solution of the homogeneous part of (13) (i.e. with $\bar{v}$ replaced by $\partial\psi_H/\partial z$ and G_u by 0), is given by

$$\bar{u}_H = \Big[\sum_{j=1}^{8} C_j \gamma_j e^{s_j y} \cos 2mz + \sum_{j=9}^{10} C_j e^{s_j y}\Big] e^{2\sigma_r t}, \tag{41}$$

where $\gamma_j = 2mPT^{\frac{1}{2}}(2\sigma_r - s_j^2 + 4m^2)$ and $s_j (j = 9, 10) = (-1)^{j+1}(2\sigma_r/P)^{\frac{1}{2}})$.

The additional constants C_9 and C_{10} are determined from the requirement that $\bar{u} = 0$ at $y = \pm\frac{1}{2}a$.

(ii) *Structure of the solutions*

Computer drawn solutions to the second-order problem are presented in figure 6. These are forced by the stationary convective cell shown in figure 5, and represent a wide range of Prandtl numbers. Absolute amplitudes are, of course, arbitrary.

We found it useful to compute the solutions separately for mechanical forcing only (G_u, G_v, G_w) and thermal forcing only (G_θ) as well as the total. As we should expect, we found that at high Prandtl numbers ($\gtrsim 10^2$) the thermal forcing completely dominates, while for low Prandtl numbers ($\lesssim 10^{-2}$) mechanical forcing dominates. In all cases, the mean meridional circulation looks like figure 6, with four cells (longitudinal rolls when viewed from above).

Figure 6(*a*), (*b*) show the induced differential rotation and temperature field for low P. We note that indeed the entire outer half of the annulus ($-\frac{1}{2}a < y < 0$) is rotating faster than Ω. We can see from (*b*) and (*f*) that the meridional circulation is everywhere thermally direct, i.e. at each level warm fluid is rising and cold sinking. Comparing (*a*) with (*f*) shows that the meridional circulation, through the Coriolis force, is 'sharpening up' the vertical shears in the differential rotation. Consistent with this, comparison of (*a*) with (*b*) indicates the differential rotation is at least qualitatively a 'thermal wind' in which positive (negative) vertical shear is associated with negative (positive) lateral temperature gradients.

In the high P case, figure 6(*c*) shows the horizontal Reynolds stress effect is wiped out, since the two halves of the annulus rotate at the same rate, on the average. Here the differential rotation is determined entirely by the thermally driven mean meridional circulation, as comparison of (*c*) with (*f*) shows. Compari-

son of (*f*) with (*d*), and (*d*) with (*c*), again shows the meridional circulation is thermally direct, and the differential rotation is a thermal wind.

At intermediate Prandtl numbers, weighted combinations of 6(*a*)–(*d*), (*f*) will represent the solutions. For example, for water, the differential rotation induced is shown in 6(*e*). The temperature field in this case is actually quite similar to 6(*d*). From 6(*e*), it is clear that even at $P = 7$ the Reynolds stresses have significant influence.

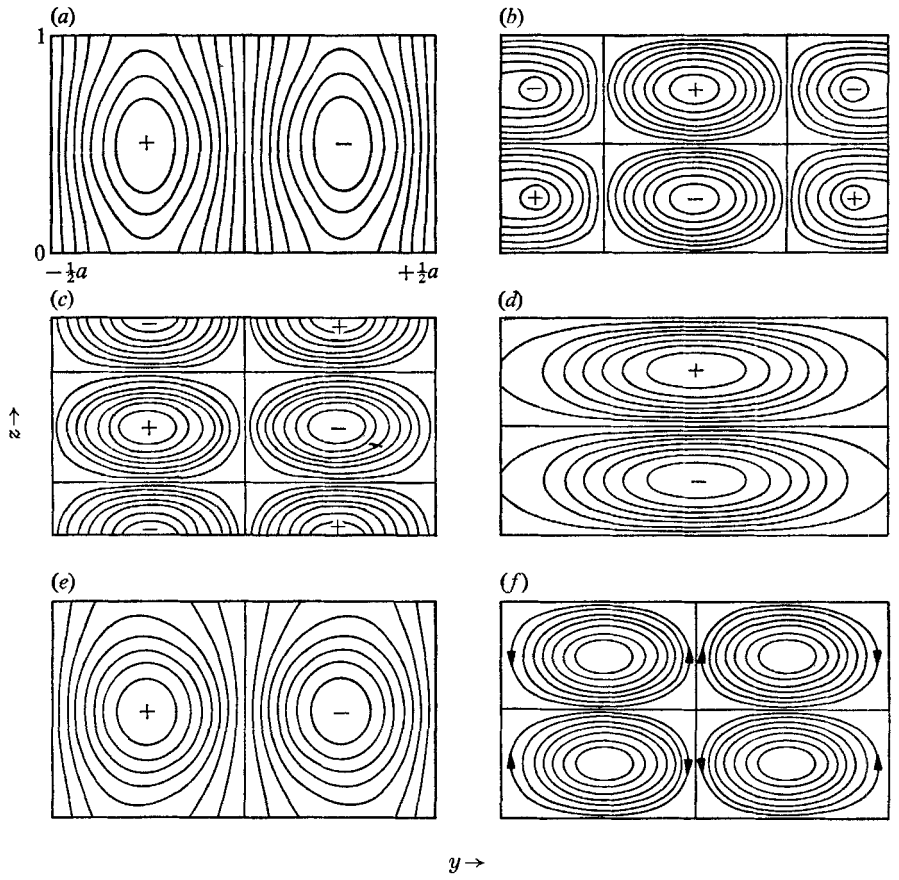

FIGURE 6. Second-order circulations and temperature forced by cell in figure 5: (*a*), (*b*) induced differential rotation and temperature, respectively, for small Prandtl number ($\lesssim 10^{-2}$); (*c*), (*d*) same for large $P(\gtrsim 10^{2})$; (*e*) differential rotation for $P = 7{\cdot}0$; (*f*) mean meridional circulation for all cases.

The four-celled meridional circulation can be shown to be present in the non-rotating case also. At high P, it is forced principally by the temperature gradient in y set up by the y variation in the vertical convergence of heat flux, which derives from the constraint that the vertical motion must vanish at the non-slip side-walls. At low P, the vertical convergence of v momentum and the lateral convergence of w momentum give a similar mean circulation.

For the aspect ratio $a = 2$ we have chosen, the differential rotation induced by

stationary convection will be qualitatively similar near R_c for all $T < \sim 2000$. This is because the inducing cell has no nodes across the annulus. However, as we showed in § 3, at higher T the most unstable linear mode has more nodes; consequently, the induced differential rotation from these will also have more structure, and will not simply be fast flowing in the outer half of the annulus. Also, of course, as T is increased for a given P, overstability will eventually set in first. Since it is unclear for overstable convection which mode or combination thereof will be selected, we do not present any details of circulations forced by them here, but they should also in general, be more complicated than the low T results.

Note added in proof. One of the writers (P. A. G.) and G. Willis have very recently observed the four longitudinal rolls superimposed on the primary transverse rolls in water in a thin non-rotating annulus with aspect ratios $a = 0{\cdot}65$ and $1{\cdot}3$ for Rayleigh numbers $\gtrsim 10000$.

The writers wish to thank Mrs Patricia Jones for programming assistance in the early stages of the work, when they were at the Department of Astro-Geophysics, University of Colorado, and Mrs Pamela Weigle, who typed the manuscript. This research was supported in part by the Air Force Cambridge Research Laboratory, Office of Aerospace Research, under contract F19628-67-C-0304.

The National Center for Atmospheric Research is supported by the National Science Foundation.

REFERENCES

Busse, F. 1970 Differential rotation in stellar convection zones. *Astrophys. J.* **159**, 629.

Chandrasekhar, S. 1961 *Hydrodynamic and Hydromagnetic Stability.* Oxford University Press.

Davies-Jones, R. P. 1970 Thermal convection in an infinite channel with no-slip sidewalls. *J. Fluid Mech.* **44**, 695.

Davies-Jones, R. P. & Gilman, P. A. 1970 On large scale solar convection. *Solar Phys.* **12**, 3.

Durney, B. 1970 Non-axisymmetric convection in a rotating spherical shell. *Astrophys. J.* (in the Press).

Goldstein, R. J. & Graham, D. J. 1969 Stability of a horizontal fluid layer with zero-shear boundaries. *Phys. Fluids*, **12**, 1133.

Greenspan, H. 1968 *The Theory of Rotating Fluids.* Cambridge University Press.

Koschmieder, E. L. 1966 On convection on a uniformly heated plane. *Beit. Phys. Atmos.* **39**, 1.

Rossby, H. T. 1969 A study of Bénard convection with and without rotation. *J. Fluid Mech.* **36**, 309.

Veronis, G. 1966 Motions at subcritical values of the Rayleigh number in a rotating fluid. *J. Fluid Mech.* **24**, 545.